Konrad-Zuse-Zentrum
für Informationstechnik Berlin

Takustraße 7
D-14195 Berlin-Dahlem
Germany

ANDREAS DRAEGERT[1]
ANDREAS EISENBLÄTTER[1]
INKEN GAMRATH[2]
AXEL WERNER[2]

Optimal Battery Controlling for Smart Grid Nodes

[1] atesio GmbH, Bundesallee 89, 12161 Berlin, Germany, {draegert, eisenblaetter}@atesio.de
[2] Zuse Institute Berlin, Department Mathematical Optimization, Takustraße 7, 14195 Berlin, Germany, {inken.gamrath, werner}@zib.de

This research has been supported by the German Federal Ministry of Economics and Technology (BMWi) within the IT2Green program (www.it2green.de)

ZIB Report 15-06 (February 2015)

Herausgegeben vom
Konrad-Zuse-Zentrum für Informationstechnik Berlin
Takustraße 7
D-14195 Berlin-Dahlem

Telefon: 030-84185-0
Telefax: 030-84185-125

e-mail: bibliothek@zib.de
URL: http://www.zib.de

ZIB-Report (Print) ISSN 1438-0064
ZIB-Report (Internet) ISSN 2192-7782

Optimal Battery Controlling for Smart Grid Nodes*

Andreas Draegert† Andreas Eisenblätter† Inken Gamrath‡

Axel Werner‡

February 2, 2015

Energy storages can be of great value when added to power grids. They introduce the possibility to store and release energy whenever this is favorable. This is particularly relevant, for example, if power supply is volatile (as is the case with renewable energy) and the network is small (so that there are few other nodes that might balance fluctuations in consumption or production). We present models and methods from mathematical optimization for computing an optimized storage schedule for this purpose. We look at alternative optimization objectives, such as smallest possible peak load, low energy costs, or the close approximation of a prescribed load curve. The optimization needs to respect general operational and economic constraints as well as limitations in the use of storage, which are imposed by the chosen storage technology. We therefore introduce alternative approaches for modeling the non-linear properties of energy storages and study their impact on the efficiency of the optimization process. Finally, we present a computational study with batteries as storage devices. We use this to highlight the trade-off between solution quality and computational tractability. A version of the model for the purpose of leveling peaks and instabilities has been implemented into a control system for an office-building smart grid scenario.

1 Introduction

The necessity of storing energy increases with the growing influence of renewable energies. This is particularly the case for consumers in a power grid who change

* This research has been supported by the German Federal Ministry of Economics and Technology (BMWi) within the IT2Green program (www.it2green.de)

† atesio GmbH, Bundesallee 89, 12161 Berlin, Germany, {draegert, eisenblaetter}@atesio.de

‡ Zuse Institute Berlin, Department Mathematical Optimization, Takustraße 7, 14195 Berlin, Germany, {inken.gamrath, werner}@zib.de

their role at times and produce energy. For them, the significance of storing energy lies in saving money by partly decoupling from the spot market and the possibility of decreasing the system usage fee (transmission fee, or wheeling charge), or—more generally—by implementing a beneficial target profile for their power in-/output from and to the grid. Besides pumped hydroelectricity systems and compressed air storage, the storage of energy in batteries is an important technology used in practice; see, for instance, [5, 9].

In this paper, we present a general model that uses an abstract representation of the physical properties of the chosen storage technology and provides an optimized storage schedule, based on given energy prices, transmission fees depending on a peak transmission, or a given target purchase profile. We also describe—as a special case—how to use the capacity of batteries to flexibly buffer energy. Here, nonlinearities have to be mastered that originate from the physics of battery storage devices. For this, there are various approaches and the more precise the physical properties are modeled, the more computationally challenging are the resulting problems. To demonstrate this, we compare different approximations of the nonlinear discharge factor under various objectives, in terms of solution quality and run-time of the solving process. An implementation of the described approach has been integrated in an operational environment to control the batteries at an ICT central office location; see `http://www.desi-it2green.de` for details.

Similar modeling approaches for optimal energy trading have been discussed in the literature, see [6, 11, 12]. These models, however, do not take detailed technical prerequisites into account. Similarly, various approaches modeling the management of residential electricity demands (see [3, 7, 14]) leave out the technical details. Besides this, literature provides—to the best of our knowledge—no comparable work that considers the computation of optimized storage schedules with a detailed view on the nonlinear technical constraints.

2 Modeling

We consider a node in a smart grid (usually a consumer, possibly a small energy producer) and assume an energy storage device, together with a controller, is available at the connection of the node to the power grid; see Figure 1 for a schematic. Using this storage device, energy for consumption or from production at the node can be buffered. This can be done for a number of reasons, such as economical ones like market prices, or environmental ones like weather conditions that influence power generation. Buffering energy, however, involves losses (which depend on the storage technology used) and in deciding when the conditions for either storing or retrieving energy are best lies the main optimization potential.

We give a mathematical model for the problem of how to find an optimal controller schedule for the storage device, and we consider various objective functions that seem reasonable in this setting. Given energy prices, the cost factor for the transmission fee, or a target purchase profile for a certain future time period, as

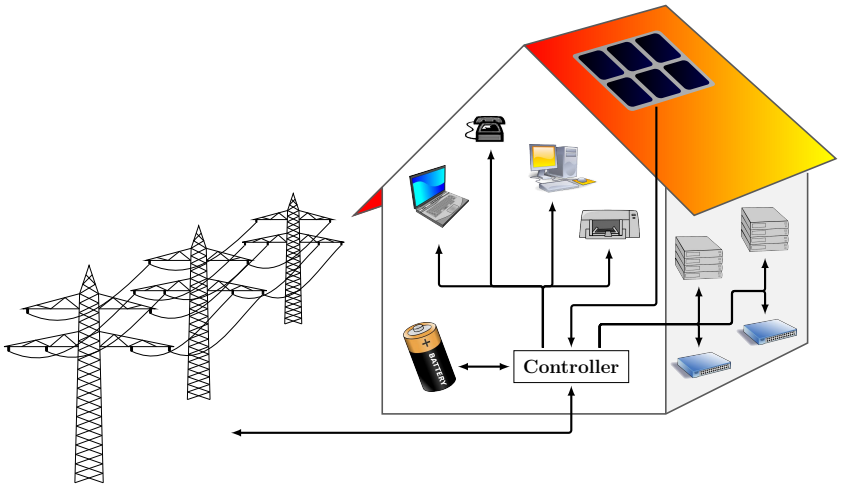

Figure 1: General setting: Energy consumed or produced at a smart grid node can be buffered using a storage device (such as a battery) with a controller

well as further input describing technological and planning properties, the model provides a schedule for storing and retrieving energy at the considered node for the said time period. To apply the model in a realistic scenario, it has to be adapted to a specific storage technology. We give an example for this in Section 3.

The model makes use of a discretization of the time scale. The optimization period $T = \{1, \dots, t_{\max}\}$ comprises a finite number of time intervals of equal length. In our computations we use time steps of 15 minutes length—corresponding to the duration of an accounting interval—and a 24 hours time horizon, so that we get $T = \{1, \dots, 96\}$. Both assumptions are obviously not limitations of the approach and finer or rougher discretization may also be used. An important consequence of the fixed time discretization is that from the model's point of view power and energy are in fixed relation: The energy E stored or retrieved within a time step is directly proportional to the power P constantly applied over this time. The conversion factor is determined by the fixed length of time steps. We therefore widely speak of energy when—in a technical sense—energy and power would have to be distinguished.

An overview of the parameters, variables and further notation used in the modeling is given in Table 1.

2.1 Storage and Purchase Schedules

Table 2 presents the part of the model that defines feasibility: Constraints (1)–(3) address energy conservation and Constraints (4)–(5) define the correct storage level. In Section 2.2, we present a choice of objective functions, some of which can be used in combination.

Similar formulations have been described in the literature [6, 11, 12], where,

Notation	Description
$T := \{1, \ldots, t_{max}\}$	set of time intervals
Parameters	
p_t, d_t	expected energy produced/demanded in time step t
S^{init}, $S^{\min}$, $S^{\max}$	initial and permissible minimal and maximal storage levels
f^{sto}, f^{ret}, f^{self}	functions modeling various energy losses
u_t^{sto}, u_t^{ret}, u_t^{buy}, u_t^{sell}	upper bounds on storing, retrieving, buying, and selling energy, respectively, in time step t
Variables	
e_t^{buy}, e_t^{sell}	energy purchased/sold in time step t
e_t^{sto}, e_t^{ret}	energy stored in/retrieved from storage in time step t
s_t	storage level in time step t
x_t	determines that energy is either stored or retrieved in time step t

Table 1: Model parameters and variables

however, none of the technical side constraints were taken into account.

Energy Conservation. The continuous variables e_t^{buy} and e_t^{sell} announce the amount of energy purchased and sold, respectively, at the spot market at time interval t. The storage schedule is given by the continuous variables e_t^{sto} and e_t^{ret}, which denote the amount of stored and retrieved energy, respectively, in each time step. Upper bounds u_t^* on the purchased, sold, stored, or retrieved energy per time step may apply, for instance, to ensure that a given peak value of purchased energy is not exceeded or the energy to be stored or retrieved is within technically prescribed limits (cf.Section 3).

The first set of energy constraints (1) guarantees that all available energy—produced, purchased, and retrieved energy—is consumed, stored, or sold. By the second and third set (2) and (3) simultaneous storing and retrieving of energy in the same time interval is forbidden (which can be seen as a restriction imposed by the modeling).

Storage. To control the total amount of stored energy, we have continuous variables s_t for the storage level in each time step, which is allowed to vary in a given range from $S^{\min}$ to $S^{\max}$. It is set to an initial value for the beginning of the optimization period by constraint (4).

The last constraint set (5) describes the change in the storage level from one time step to the next. The functions f^{self}, f^{sto}, and f^{ret} determine the impact of losses that arise from self-discharging, storing, and retrieving energy over a time interval in dependence of the storage level s at the beginning of this time interval:

- $f^{\text{self}}(s) \in [0,1]$ defines the fraction of energy remaining after losses due to self-discharging

Energy conservation

$$e_t^{\text{buy}} + p_t + e_t^{\text{ret}} = e_t^{\text{sell}} + d_t + e_t^{\text{sto}} \qquad \forall t \in T \tag{1}$$

$$e_t^{\text{sto}} - x_t u_t^{\text{sto}} \leq 0 \qquad \forall t \in T \tag{2}$$

$$e_t^{\text{ret}} - (1 - x_t) u_t^{\text{ret}} \leq 0 \qquad \forall t \in T \tag{3}$$

Storage

$$s_0 = S^{\text{init}} \tag{4}$$

$$s_t = s_{t-1} f^{\text{self}}(s_{t-1}) + e_t^{\text{sto}} f^{\text{sto}}(e_t^{\text{sto}}, s_{t-1}) - e_t^{\text{ret}} f^{\text{ret}}(e_t^{\text{ret}}, s_{t-1}) \qquad \forall t \in T \tag{5}$$

Variables

$$e_t^{\text{buy}} \in [0, u_t^{\text{buy}}] \qquad \forall t \in T$$

$$e_t^{\text{sell}} \in [0, u_t^{\text{sell}}] \qquad \forall t \in T$$

$$e_t^{\text{sto}} \in [0, u_t^{\text{sto}}] \qquad \forall t \in T$$

$$e_t^{\text{ret}} \in [0, u_t^{\text{ret}}] \qquad \forall t \in T$$

$$s_t \in [S^{\min}, S^{\max}] \qquad \forall t \in T \cup \{0\}$$

$$x_t \in \{0, 1\} \qquad \forall t \in T$$

Table 2: General Model for computing a storage schedule

- $f^{\text{sto}}(s, e^{\text{sto}}) \in [0, 1]$ describes the fraction of energy remaining after losses in the charging process (assuming a fixed charging scheme over the time interval)
- $f^{\text{ret}}(s, e^{\text{ret}}) \geq 1$ specifies the discharge factor; more precisely, the quotient of discharged energy, the amount by which the storage level is reduced, and retrieved energy, usable after discharging (assuming a constant discharging current over the time interval).

The nature of these functions depends on the used storage technology and has a decisive influence on the mathematical type of the model, as well as its solvability; see Section 3 for a more detailed discussion.

Miscellaneous. Further restrictions can be added to the model that allow the application of the optimization model in various scenarios.

When applying the optimization in a repetitive pattern, controlling the *final storage level*

$$s_{t_{\max}} \geq S^{\text{fin}}$$

at the end of the present time horizon may be desired. This allows to avoid schedules in which the stored energy is completely used up towards time $t_{\max}$. Similarly, the battery level at the end of the optimization period might be required to reach a specific value for reasons such as planned maintenence.

Solutions that buy and sell energy at the same time may be undesired and forbid-

den:

$$e_t^{\text{buy}} - y_t u_t^{\text{buy}} \leq 0, \quad e_t^{\text{sell}} - (1-y_t) u_t^{\text{sell}} \leq 0 \qquad \forall t \in T$$

where $y_t \in \{0,1\}$ determines that we either buy or sell energy at the spot market. Note that, in case energy costs are minimized (see Section 2.2) and buying energy is more expensive than selling energy, these constraints are redundant for optimality.

Additional parameters for these restrictions as well as for the different objective functions are given in Table 3.

Notation	Description
t_{max}	last time interval of the optimization horizon
Parameters	
S^{fin}	final storage level
Objective coefficients	
c_t^{buy}, c_t^{sell}	cost/revenue of trading energy in time step t
E^{peak}	current peak transmission before actual optimization horizon
c^{peak}	cost factor for transmission fee
a_t^{buy}, a_t^{sell}	value for time step t in a desired purchase/selling profile
Variables	
y_t	determines that energy is either purchased or sold at the spot market in time step t

Table 3: Additional model parameters and variables for further restrictions and objective functions

2.2 Objectives

The constraints given in Section 2.1 define a *feasible schedule* for the considered time horizon. Optimization itself consists now of finding a feasible schedule that is *optimal* with respect to a certain objective function. In the following, we list some objectives z that we considered. Each optimization problem can be formulated as a minimization problem, hence we are always looking for a feasible schedule that minimizes z.

Minimization of Energy Costs. Given spot market prices $c_t^{\text{buy}} \in \mathbb{R}$ and $c_t^{\text{sell}} \in \mathbb{R}$ for buying and selling energy at time t, respectively, the objective is to minimize the total energy cost

$$z(e_t^{\text{buy}}, e_t^{\text{sell}}) = \sum_{t \in T} \left(c_t^{\text{buy}} e_t^{\text{buy}} - c_t^{\text{sell}} e_t^{\text{sell}} \right).$$

Minimization of Peak Power. In some applications, the transmission fee (or wheeling charge) depends on the peak power, which is the highest annual mean

($4 \max e_t^{\text{buy}}$). Then, minimizing the maximal load can be of interest:

$$z(e_t^{\text{buy}}) \;=\; \max_{t \in T} e_t^{\text{buy}}.$$

When the time horizon of an individual optimization run is shorter than one year, the objective for such runs can account for the increment of the peak value during the time horizon. The peak attained at earlier runs is propagated using a parameter E^{peak}. The objective then reads as

$$z(e_t^{\text{buy}}) \;=\; \max\left(0, \max_{t \in T}\left(e_t^{\text{buy}} - E^{\text{peak}}\right)\right).$$

Minimization of Combined Costs for Energy Purchase and Peak Consumption. The above objectives can be combined. Given the cost factor for the transmission fee $c^{\text{peak}} \in \mathbb{R}$, the objective to minimize the total cost[1] is

$$z(e_t^{\text{buy}}, e_t^{\text{sell}}) \;=\; c^{\text{peak}} \cdot \max_{t \in T} e_t^{\text{buy}} + \sum_{t \in T}\left(c_t^{\text{buy}} e_t^{\text{buy}} - c_t^{\text{sell}} e_t^{\text{sell}}\right).$$

As above, minimizing energy above a given "allowed" peak value might provide a better objective for consecutive optimization runs over a long time period.

Approximation of a Favored Purchase Profile. To minimize the deviation from a target profile for traded energy, given by values $a_t^{\text{buy}}, a_t^{\text{sell}} \geq 0$ for the considered time steps $t \in T$, we can formulate the objective

$$z(e_t^{\text{buy}}, e_t^{\text{sell}}) \;=\; \sum_{t \in T}\left(|e_t^{\text{buy}} - a_t^{\text{buy}}| + |e_t^{\text{sell}} - a_t^{\text{sell}}|\right).$$

3 Optimizing Battery Charging and Discharging Schedules

In Section 2, we presented a mathematical model for admissible charging/discharging and purchase schedules, as well as some examples for objective functions that have been used in practice. All details concerning physics and technology of the used storage device are hidden in the functions f^{self}, f^{sto}, and f^{ret}. Depending on those functions the nature of the model, as well as the available algorithmic tools for solving it, may vary largely.

This section gives an example how to make the general model precise for a specific situation. We consider one in which the storage device is a battery of total

[1] Scaling factors for the different terms may apply to account for the highly differing time scales involved: whereas the optimization period is usually only one day, the transmission fees are computed based on the consumption in a full year, which makes it difficult to arrive at comparable cost values.

capacity Q. We emphasize that the specialization discussed in this section constitutes a rather rough version of a battery model and more realistic models can be implemented. Indeed, the level of detail of the technological model can be traded off against its solvability; we demonstrate this in the following by comparing the solutions and run-times using different possibilities for modeling the discharging factor f^{ret}.

3.1 Modeling the Discharging Loss

For the sake of a pointed explanation, we focus on the discharging loss function f^{ret} and assume constant functions f^{self} and f^{sto} for self-discharging and charging, respectively. For the discharging loss we consider a strictly monotonically increasing functions $f^{\text{ret}} : \mathbb{R}_{\geq 0} \to \mathbb{R}_{\geq 1}$ only depending on the amount of retrieved energy e_t^{ret}. Under these conditions, the discharging factor can be expressed analytically as follows (see, for instance, [8, 10]):

$$f^{\text{ret}}(e_t^{\text{ret}}) = 1 + \frac{c\left(1 - e^{-kg(e_t^{\text{ret}})}\right)}{kg(e_t^{\text{ret}})},$$
$$e_t^{\text{ret}} = \frac{Qk}{4c\left(1 - e^{-kg(e_t^{\text{ret}})}\right) + 4kg(e_t^{\text{ret}})},$$

where Q is the maximum capacity (at infinitesimal current), k is a constant rate, and c is the gap between available charge capacity and total capacity. Moreover, g is an implicitly given auxiliary function, which cannot be described elementarily. The resulting curve of the function f^{ret} is illustrated in Figure 2 (solid black line).

Exact Loss Function. Including the exact nonlinear function directly yields a model which is algorithmically hard to solve. Heuristics can be used to improve solvability. To find start solutions, the variables e_t^{ret} can be fixed to either 0 or values depending on the energy costs or the former peak transmission, and the resulting easier (linear) problem can be solved. For improving solutions, a local neighborhood search can be applied to the values of e_t^{ret} of the current best solution.

Constant Loss Factor. The roughest way to avoid the nonlinearity is to approximate the function with a constant. Then, we have the same loss factor for each time step, independent of the amount of discharged energy. A special case of this approximation is to use $f^{\text{ret}} \equiv 0$, this is, we assume no losses when discharging the battery.

This constant approximation is the most commonly used discharging loss in the literature, see [6, 11, 12].

Iterative Solution with Constant Loss. It is possible to avoid the nonlinearity in the first place by using a constant loss f_t^{ret} for each time step t. In this case

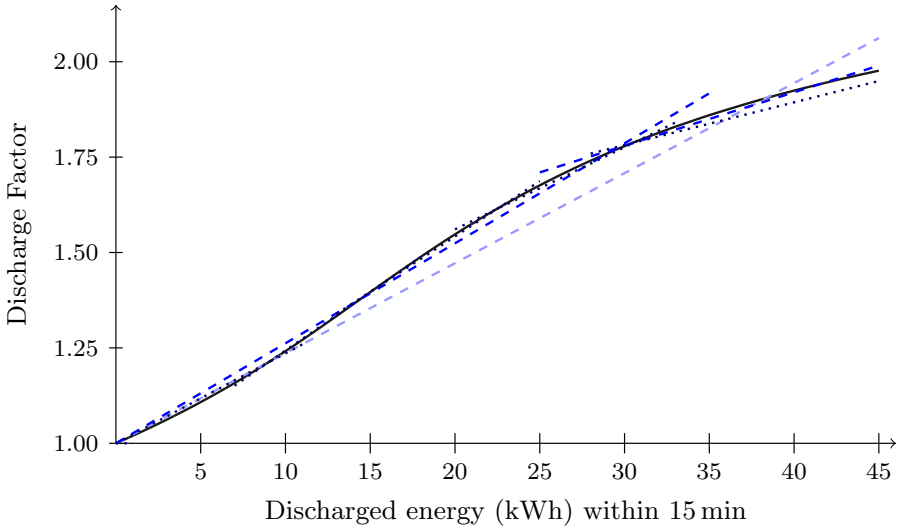

Figure 2: Discharge factor f^{ret} with respect to the discharging rate at constant potential (black) and linearizations by an affine (light blue dashed), a concave, piecewise linear function (dark blue dashed), and a nonconvex, nonconcave, piecewise linear function (dark blue dotted)

the values f_t^{ret} used for the optimization potentially deviate strongly from the real loss. The optimization model is solved repeatedly until a given maximal number of iterations is reached. After each iteration the new solution is used to update the constants f_t^{ret} according to the correct loss. Additionally, the variables e_t^{ret} are bounded depending on their value in the new solution and the former bounds.

Affine and Piecewise Linear Approximation. A finer way of approximating f^{ret} is to use an affine, continuous, concave, piecewise linear, or a continuous, nonconvex, nonconcave, piecewise linear function. All of these variants result in a quadratic or polynomial model, in which the difference between the computed and the real loss corresponds to the gap between the nonlinear discharging factor and the approximation.

These approximations of the nonlinear functions are illustrated in Figure 2. The light blue dashed line is the affine linear approximation, the dark blue dashed is the affine, continuous, concave, piecewise linear one, and the dark blue dotted line is the continuous, nonconvex, nonconcave, piecewise linear approximation.

Since the approximated versions of the discharge functions do not model the discharge exactly, it is possible that the obtained schedules slightly violate the exact side constraints. Therefore, in a postprocessing step violations, such as a load level of more than 100 % or less than the allowed minimal level, are repaired and correctness with respect to the exact constraints is ensured.

Parameter	Value
$t_{\max}$	96
$S^{\max}$	360 kWh
$S^{\min}$	180 kWh
S^{init}	252 kWh
u^{buy}	∞
u^{sell}	∞
u^{ret}	45 kWh
u^{sto}	9 kWh
f^{sto}	0.9
f^{self}	0.9995
Q	436.51
k	0.6750
c	1.4363

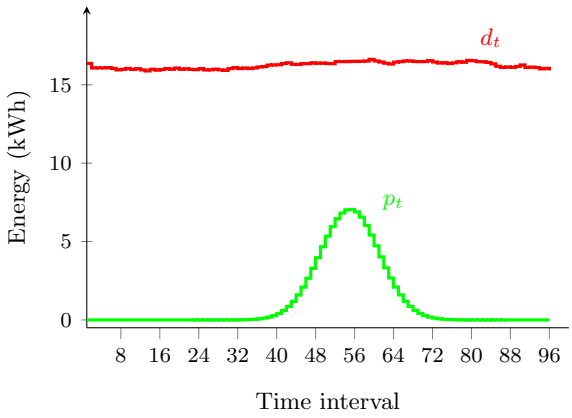

Table 4: Parameter values used for the computations (left), produced energy from solar panels (green) and demanded energy (red) in each time step for an exemplary sunny day (right).

The usage of the exact discharge loss function results in a mixed integer nonlinear program (MINLP) that has to be solved, whereas the various approximations lead to mixed integer quadratic programs (MIQP)—or can at least be reformulated as such—or even to mixed integer linear programs (MILP). These models can be solved with a suitable optimization software, such as SCIP [1, 13][2]. Usually, the solution process involves solving a linear relaxation and then continuing in a branch-and-bound phase, where a branch-and-bound tree is implicitly generated whose nodes correspond to suitable subproblems. For more details on branch-and-bound see, for instance, [2, 4].

To speed up the computation, an early termination strategy can be used, where the solving process is stopped after 1000 branch-and-bound nodes of stalling, i. e., nodes without an improvement upon the best obtained solution so far. This solution is possibly not optimal, but in general it can be expected that continuing the solving process does not lead to better solutions in a reasonably short time.

In the following, we compare these different approaches with respect to solvability (run-time) and quality of the solution. The parameter values used for the computations are given in Table 4 and are suited to model the scenario of a small ICT central office location.

[2] see `http://scip.zib.de`

3.2 Case Study: Optimizing Energy and Transmission Costs

We consider an example where we minimize both energy costs and peak increase. The target peak transmission was set to 80 kW. Energy prices are taken from the European electricity spot market EEX in Leipzig.[3] Net demand—consumed energy at the node minus the produced amount of energy—decreases during the day, due to electricity produced by solar panels during daylight. Figure 3 illustrates a schedule for charging/discharging and trading energy on an exemplary day.

3.3 Computational Study

In this section we report on computational studies. On the one hand, we pick each of the four objectives presented in Section 2.2, on the other hand, we try out each of the solution approaches discussed in Section 3.1. Each of these combinations is applied to 60 instances. Our findings are reported below.

Every instance represents a whole day (from 0:00 to 24:00). The consumer's energy demand is assumed to be composed of the consumption of two types of electrical devices:

- permanently powered devices—constantly running hardware such as ICT equipment at a central office or fridges at a household
- daylight devices—such as lights, personal computers or general household appliances that are usually switched off during the night

The set of the 60 test instances is partitioned into three equal-sized sets, each containing instances of one of the following category:

- producers with hardware of both of the above types and a varying energy-production over day (standard smart grid nodes)
- non-producers with both types of devices, but without energy-production (standard power-consuming locations)
- non-producers with flexible power consumption for the permanently powered devices (the role model for such locations being future central office sites with load-adaptive ICT equipment)

The various power consumptions of the devices might depend on the type of day (working or weekend day), the outside temperature, and the production depends on the sunshine duration of the day. Twenty randomly chosen days throughout the course of the year 2011 have been considered, each with historic data on temperatures and energy prices from the European electricity spot market EEX.

Table 5 lists numerical results. Over the 60 computations for each combination of objective (described in the table header) and solution method (described in bold-

[3] see `http://www.eex.com/en#/en`

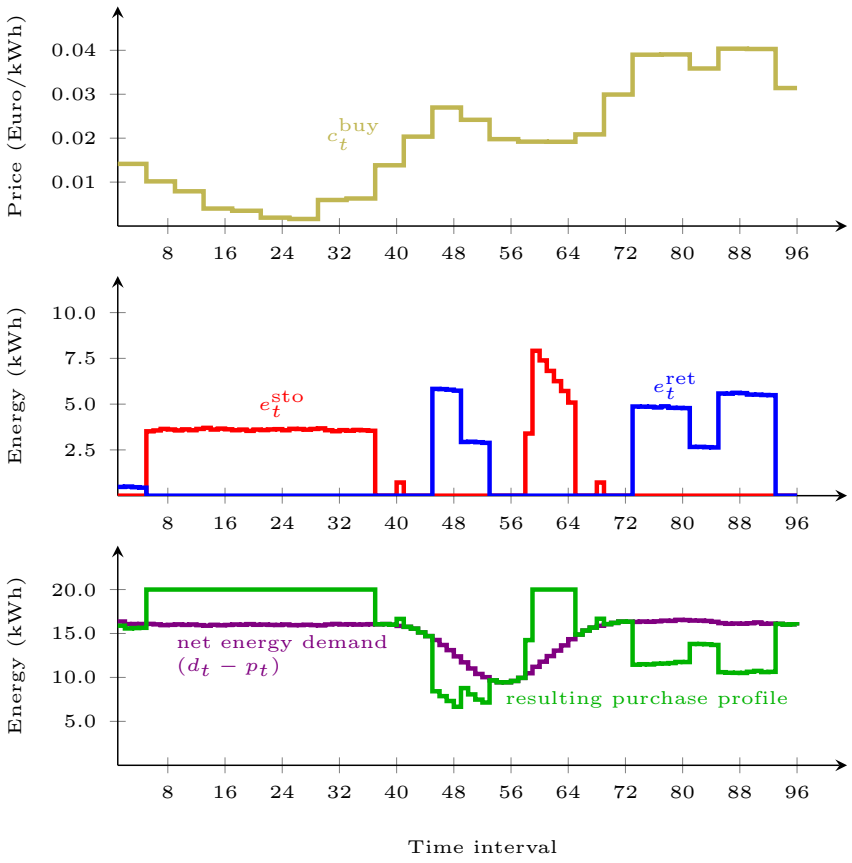

Figure 3: Optimal schedule for the example day: Energy prices (top), amount of energy stored in/retrieved from the battery (middle), and net energy demand and resulting energy purchase profile (bottom).
Energy is stored in the battery (red curve) during the night and over two hours in the afternoon, when prices are low, and retrieved to power the site (blue curve), when prices are higher. At the same time, the increase over the preset peak value of 80 kW (corresponding to 20 kWh of energy in every quarter hour) is aimed to be kept small—indeed, the resulting purchase profile shows that the peak is not increased at all, i. e., too high peaks in the purchase profile are shaved off.
The impact of the physical properties of the battery and their modeling can also be read off from the figure. Due to the energy losses involved, the integral of the red curve (the total stored energy) is greater than the integral of the blue curve (total retrieved energy). The more precise the used technical constraints model the losses, the more reliable is the resulting schedule. Furthermore, a higher discharge curve yields an even greater difference of these integrals, due to the increasing discharge loss function; hence high discharge peaks are avoided: in this example the discharged energy in every quarter hour is always significantly below the maximally allowed value of 45 kWh (cf. Table 4).

face), shifted geometric means[4] of the running times and the objective values of the repaired solutions were taken. Each individual computation was carried out with a time limit of 300 seconds, using the solver SCIP [1] on a Linux system (in 64 bit mode) running on an 8-core Intel Xeon E5420 2.5 GHz CPU with 6 MiB cache and 16 GiB RAM (each run made use of only one core). For comparison, the topmost section shows the mean value of the respective objectives for the 0-schedules for each case, i. e., no battery activity is taking place.

The first observation is that the early termination strategy has no influence on the iterative approach, since during the solution of the resulting, relatively easy MIP the branch-and-bound tree does not get large enough to even produce 1000 nodes in total. The same happens for the constant approximations, except when aiming at a given target profile. In the latter case, we have to deal with a nonlinear objective that contains absolute values, which blows up the model to some extent when reformulated as a MILP. In all other cases, early termination significantly reduces the run-times without causing much deterioration in solution quality.

A comparison of the approaches leaves the linear approximations with few (in this case, 2) affine functions, the completely linear approximation, and—at least for the first three objectives—the iterative approach as the generally favourable methods. In conjunction with early termination, all of these yield the best solutions in acceptable run-times of at most a few seconds. This is fast enough so that the model can be used in a rolling-horizon implementation, where it has to be resolved periodically after suitable time intervals, such as 15 minutes.

Using the exact loss function or approximations with many affine functions leads to worse solutions for a short time limit or after early termination. For obtaining better or even optimal solutions for these more precise, but also harder to solve model variants, longer run-times would be necessary. On the other hand, the constant approximation variants can be solved very fast, but largely result in solutions of comparable (mediocre) quality as the exact and very precisely approximated versions.

We remark that due to the postprocessing necessary for the approximation variants, the final (repaired) solutions for early termination might have a slighty better objective value than the best solutions found in the optimization run itself; in Table 5 this even shows in the mean value for the constant approximation approach minimizing the deviation from a target profile.

[4]The shifted geometric mean of n values $a_1, \ldots, a_n \geq 0$ is defined as

$$\left(\prod_{i=1}^{n} (a_i + s) \right)^{\frac{1}{n}} - s,$$

where $s > 0$ is a sufficiently small shift parameter.

Objective:	Energy costs (€)		Peak power increase (kW)		Total costs (€)		Target profile (total deviation)	
Without optimization								
Solution	76.831		8.342		100.157		317.037	
Exact function for discharge factor								
Best Solution	75.800		2.934		85.579		192.158	
Time (out)	300.000	(60)	2.781	(4)	283.374	(59)	300.000	(60)
Early termination	75.800		2.934		85.579		192.538	
Time (out)	11.631	(0)	0.552	(0)	12.988	(0)	14.632	(0)
Piecewise linear approximation of discharge factor by 5 affine functions								
Best Solution	76.054		2.765		84.390		177.786	
Time (out)	300.000	(60)	2.725	(2)	300.000	(60)	300.000	(60)
Early termination	76.056		2.934		85.784		182.362	
Time (out)	38.123	(0)	1.456	(0)	34.798	(0)	47.362	(0)
Piecewise linear approximation of discharge factor by 2 affine functions								
Best Solution	75.008		2.608		83.076		167.396	
Time (out)	20.722	(7)	0.741	(1)	16.420	(5)	108.351	(38)
Early termination	75.008		2.608		83.076		172.083	
Time (out)	4.274	(0)	0.187	(0)	5.577	(0)	5.542	(0)
Linear approximation of discharge factor								
Best Solution	75.005		2.605		83.059		168.080	
Time (out)	25.128	(10)	0.743	(1)	19.860	(7)	120.954	(42)
Early termination	75.005		2.605		83.060		173.489	
Time (out)	4.200	(0)	0.201	(0)	5.839	(0)	5.724	(0)
Iterative solution with constant discharge factor								
Best Solution	75.092		2.631		83.136		190.337	
Time (out)	0.715	(0)	0.419	(0)	0.761	(0)	58.242	(0)
Early termination	75.092		2.631		83.136		190.337	
Time (out)	0.748	(0)	0.437	(0)	0.799	(0)	58.239	(0)
Constant approximation of discharge factor								
Best Solution	76.374		2.631		84.346		175.798	
Time (out)	0.126	(0)	0.109	(0)	0.234	(0)	41.054	(20)
Early termination	76.374		2.631		84.346		175.763	
Time (out)	0.128	(0)	0.101	(0)	0.249	(0)	3.700	(0)
Zero discharge factor								
Best Solution	77.008		3.175		85.321		176.826	
Time (out)	0.138	(0)	0.105	(0)	0.291	(0)	32.961	(12)
Early termination	77.008		3.175		85.321		176.823	
Time (out)	0.138	(0)	0.098	(0)	0.304	(0)	4.895	(0)

Table 5: Computational results for the different solution methods with four different objectives: shifted geometric means over 60 instances of objective values of best obtained solutions and best solutions obtained after stalling, as well as run-times for the respective solution processes (and number of runs in each section that hit the time limit of 300 seconds)

4 Conclusion and Outlook

We have presented a flexible approach based on mathematical optimization for computing optimal schedules for trading and buffering energy in a smart grid. We have applied the approach to a smart grid scenario, using batteries as storage devices. The techniques have been successfully implemented into a control system for a smart grid node, optimizing storage schedules every 15 minutes.

We studied alternative objective functions, such as minimization of costs or deviation from a target load profile. By varying the level of detail in modeling technical constraints, we observe a trade-off between solvability of the model and the quality of solutions.

The presented model can be extended in various ways. Additional constraints can be incorporated, accounting for maintenance of the storage device and special contracts with power suppliers. Future extensions may address the involvement in the trade of operating reserve electricity and other storage technologies, such as pumped-storage hydroelectricity.

Acknowledgments

This work was supported by the German Federal Ministry of Economics and Energy (BMWi) within the DESI project (led by the Telekom Innovation Laboratories) as part of the IT2Green framework (`it2green.de`). The authors thank Dr. Heiko Lehmann (Telekom Innovation Laboratories) for his support and guidance.

References

[1] Tobias Achterberg. SCIP: solving constraint integer programs. *Mathematical Programming Computation*, 1(1):1–41, 2009.

[2] Tobias Achterberg, Thorsten Koch, and Alexander Martin. Branching rules revisited. *Operations Research Letters*, 33(1):42–54, 2005.

[3] A. Barbato and G. Carpentieri. Model and algorithms for the real time management of residential electricity demand. *Energy Conference and Exhibition (ENERGYCON)*, pages 701–706, 2012.

[4] R. J. Dakin. A tree-search algorithm for mixed integer programming problems. *The Computer Journal*, 8(3):250–255, 1965.

[5] Bruce Dunn, Haresh Kamath, and Jean-Marie Tarascon. Electrical energy storage for the grid: A battery of choices. *Science*, 334(6058):928–935, 2011.

[6] Lazaros Exarchakos, Matthew Leach, and Georgios Exarchakos. Modelling electricity storage systems management under the influence of demand-side management programmes. *International Journal of Energy Research*, 33:62–76, 2009.

[7] Matteo Fischetti, Giorgio Sartor, and Arrigo Zanette. A MIP-and-refine matheuristic for smart grid energy management. *International Transactions in Operational Research*, 22(1):49–59, 2015.

[8] M. R. Jongerden and B. R. Haverkort. Which battery model to use? *IET Software*, 3(6):445–457, 2009.

[9] J. Kondoh, I. Ishii, H. Yamaguchi, A. Murata, K. Otani, K. Sakuta, N. Higuchi, S. Sekine, and M. Kamimoto. Electrical energy storage systems for energy networks. *Energy Conversion & Management*, 41:1863–1874, 2000.

[10] James F. Manwell, Jon G. McGowan, Utama Abdulwahid, and Kai Wu. Improvements to the hybrid2 battery model. In *Windpower 2005 Conference*. American Wind Energy Association, 2005.

[11] T. Sousa, H. Morais, Z. Vale, P. Faria, and J. Soares. Intelligent energy resource management considering vehicle-to-grid: A simulated annealing approach. *IEEE Transactions on Smart Grid*, 3(1), 2012.

[12] Petr Stluka, Datta Godbole, and Tariq Samad. Energy management for buildings and microgrids. *50th IEEE Conference on Decision and Control and European Control Conference (CDC-ECC)*, 2011.

[13] Stefan Vigerske. *Decomposition of Multistage Stochastic Programs and a Constraint Integer Programming Approach to Mixed-Integer Nonlinear Programming*. PhD thesis, Humboldt-University Berlin, 2013.

[14] Di Zhang, Lazaros G. Papageorgiou, Nouri J. Samsatli, and Nilay Shah. Optimal scheduling of smart homes energy consumption with microgrid. *1st International Conference on Smart Grids, Green Communications and IT Energy-aware Technologies*, 2011.